

Straight nodal-line phonons in symmorphic space groups

Guang Liu,^{1,2} Yuanjun Jin,^{1,2} Zhongjia Chen,^{1,2,3} and Hu Xu^{1,2,*}

¹*Department of Physics & Institute for Quantum Science and Engineering, Southern University of Science and Technology, Shenzhen 518055, P. R. China.*

²*Guangdong Provincial Key Laboratory of Computational Science and Material Design, Southern University of Science and Technology.*

³*Department of Physics, South China University of Technology, Guangzhou 510640, P. R. China*

Based on first-principles calculations and effective model analysis, all possible straight nodal-line phonons in symmorphic space groups are uncovered. A classification of two-band $\mathbf{k} \cdot \mathbf{p}$ models at an arbitrary point on the nodal lines is carried out, and these nodal-line phonons are found to locate along the high symmetry lines of the Brillouin zone. According to our classification, there are two types of nodal-line phonons in symmorphic space groups. The first type possesses a linear dispersion perpendicular to the nodal lines, while the second type exhibits a quadratic dispersion. The underlying mechanisms are revealed by symmetry analysis, and the types of nodal-line phonons can be distinguished through the little group of the high symmetry lines. Our work not only classifies nodal-line phonons but also provides guidance to search for topological nodal lines in bosonic systems.

INTRODUCTION

Topological quantum states have attracted much attention in current condensed-matter physics and materials physics [1–3]. Topological semimetal is a new class of quantum materials that possesses stable band crossings near the Fermi energy, resulting in many promising properties, such as negative magnetoresistance, chiral magnetic effect, anomalous Hall effect. According to the dimension of the band nodes in the Brillouin zone (BZ), these peculiar crossings can be divided into zero-dimensional nodes[4–6], one-dimensional nodal rings and lines[7–14], and two-dimensional nodal surfaces[15–17]. Topological nodal-line (NL) semimetal has various ways of band touching along one-dimensional curves in momentum space. The classification of these nodal lines in electronic systems are so far mainly based on band energy degeneracy, band dispersion, and nodal line shape. However, electrons are fermions, which are limited by the Pauli exclusion principle, leading to limited NLs near the Fermi level in electron systems.

Besides electrons, phonons are another important elementary excitations in condensed-matter physics. The concept of topology has recently been introduced into phonon systems, greatly enriching the physics of symmetry-protected topological states[18–29]. Topological phonons have potential applications in electron-phonon coupling, multiphonon process, and thermal transports. Besides, phonons are bosons, so the entire frequency range of the phonon spectrum can be physically observed, which can provide us with more material samples to improve the classification of topological NLs. Very recently, nontrivial topological NL phonons in crystalline solids have been studied, including helical NLs in MoB₂[30], light operated NL phonons in oxide perovskites[31], and Weyl nodal straight line phonons in MgB₂[32]. However, these works focus only on the re-

search of the NLs in a certain kind of material. There still lacks an extensive classification of the NLs in the phonon systems.

In this work, the NL phonons are classified according to the order of the phonon band dispersion relation in the plane perpendicular to the NL. To explore this, a systematic symmetry analysis of the high-order NLs in 73 symmorphic space groups is performed, and all possible straight NLs along the high symmetry lines are listed in Table I. It is found that the linear nodal line(LNL) is protected by the point group symmetry $C_3 + \mathcal{PT}$ or C_{3v} . Quadratic nodal line(QNL) is protected by one of eight symmetries: $C_2 + \mathcal{S}_4\mathcal{T}$, $C_{2v} + \mathcal{S}_4\mathcal{T}$, $C_3 + M_z\mathcal{T}$, $C_{3v} + M_z\mathcal{T}$, $C_4 + \mathcal{PT}$, C_{4v} , $C_6 + \mathcal{PT}$, and C_{6v} . It should be noted that the above-mentioned symmetries in the form $A + B$ represent a point group symmetry plus an operation, i.e., the former represents the little group corresponding to the nodal line, and the latter represents the symmetry operation that needs to be satisfied after considering the time reversal symmetry (\mathcal{T}).

RESULTS AND DISCUSSION

To understand the properties of the NL phonons, we first show the nodal-line solution in terms of the two-band $\mathbf{k} \cdot \mathbf{p}$ effective Hamiltonian. Generally, the crossings of two phonon branches can be described by a 2×2 effective Hamiltonian, namely

$$H(\mathbf{q}) = d(\mathbf{q})\sigma_+ + d^*(\mathbf{q})\sigma_- + f(\mathbf{q})\sigma_z \quad (1)$$

where H is referenced to the frequency of an arbitrary point on the NL phonon, $d(\mathbf{q})$ represents a complex function, $f(\mathbf{q})$ represents a real function, \mathbf{q} denotes the wave vector which is restricted to the plane perpendicular to the NL, $\sigma_{\pm} = \sigma_x \pm i\sigma_y$, and $\sigma_{0,x,y,z}$ are the Pauli matrices. The leading order of $d(\mathbf{q})$ and $f(\mathbf{q})$ determine the

Table I: Linear nodal lines and quadratic nodal lines in symmorphic space groups and their corresponding symmetries.

line type	symmetry	location	Nodal line	symmetry	location	
Linear	$C_3 + \mathcal{PT}$	147 (0,0,w)	Quadratic	$C_{2v} + \mathcal{S}_4\mathcal{T}$	111 (0,0,w)	
		147 (1/3,1/3,w)			111 (1/2,1/2,w)	
		148 (w,w,w)			115 (1/2,1/2,w)	
		164 (1/3,1/3,w)			115 (0,0,w)	
		175 (1/3,1/3,w)			119 (w,w,-w)	
		200 (w,w,w)			121 (w,w,-w)	
		202 (w,w,w)			215 (1/2,1/2,w)	
		204 (w,w,w)			215 (0,w,0)	
	C_{3v}	156 (0,0,w)			216 (w,w,0)	
		157 (0,0,w)			217 (w,-w,w)	
		157 (1/3,1/3,w)			$C_3 + M_z\mathcal{T}$	174 (0,0,w)
		157 (-1/3,-1/3,w)			$C_{3v} + M_z\mathcal{T}$	187 (0,0,w)
		160 (w,w,w)			189 (0,0,w)	
		162 (0,0,w)			$C_4 + \mathcal{PT}$	83 (0,0,w)
		162 (1/3,1/3,w)				83 (1/2,1/2,w)
		164 (0,0,w)				87 (w,w,-w)
		166 (0,0,w)			C_{4v}	99 (0,0,w)
		183 (1/3,1/3,w)				99 (1/2,1/2,w)
		189 (1/3,1/3,w)				107 (w,w,-w)
		189 (-1/3,-1/3,w)				123 (0,0,w)
		191 (1/3,1/3,w)				123 (1/2,1/2,w)
		215 (w,w,w)				139 (w,w,-w)
		216 (w,w,w)				221 (1/2,1/2,w)
		217 (w,w,w)				221 (0,w,0)
		221 (w,w,w)				225 (w,w,0)
		225 (w,w,w)				229 (w,-w,w)
229 (w,w,w)	$C_6 + \mathcal{PT}$	175 (0,0,w)				
Quadratic	$C_2 + \mathcal{S}_4\mathcal{T}$	81 (0,0,w)	C_{6v}	183 (0,0,w)		
				191 (0,0,w)		

classification of NLs. If the leading orders of $d(\mathbf{q})$ and $f(\mathbf{q})$ are linear, the nodal line can be named as LNL. By analogy, we can define the QNL.

Linear nodal line

As listed in Table I, the LNL phonons are stabilized by symmetry C_{3v} or $C_3 + \mathcal{PT}$. For little group C_{3v} , there is a two-dimensional irreducible representation corresponding to a double degenerate NL. An arbitrary point on this path is invariant under the little group which contains two generators: the threefold rotation C_{3z} and vertical mirror M_x . The relevant representation is Γ_3 , of which the basis functions are $\{(\mathbf{S}_x - i\mathbf{S}_y), -(\mathbf{S}_x + i\mathbf{S}_y)\}$. The matrix representations of the generators can be expressed in the above basis as

$$D(C_{3z}) = e^{2i\sigma_z\pi/3}, D(M_x) = \sigma_x. \quad (2)$$

The Hamiltonian is constrained by the symmetry transformations, namely

$$D(R)H_{eff}(\mathbf{q})D^{-1}(R) = H_{eff}(R\mathbf{q}), \quad (3)$$

where R denotes the corresponding operator C_{3z} and M_x , which acts on \mathbf{q} . The constraint Eq. (3) gives

$$\begin{aligned} f(q_+, q_-) &= f(e^{i2\pi/3}q_+, e^{-i2\pi/3}q_-), \\ e^{i4\pi/3}d(q_+, q_-) &= d(e^{i2\pi/3}q_+, e^{-i2\pi/3}q_-), \\ -f(q_+, q_-) &= f(-q_-, -q_+), \\ d^*(q_+, q_-) &= d(-q_-, -q_+), \end{aligned} \quad (4)$$

where $q_{\pm} = q_x \pm iq_y$. Then we expand Eq. (4) and remain the lowest orders as

$$\begin{aligned} f(\mathbf{q}) &= a_1(q_+^3 + q_-^3), \\ d(\mathbf{q}) &= ia_2q_-, \end{aligned} \quad (5)$$

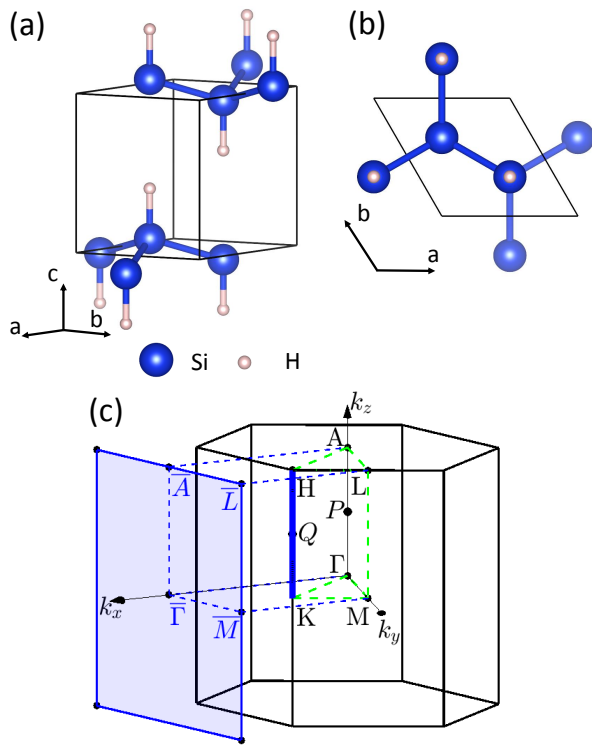


FIG. 1: Crystal structure and the corresponding BZ. (a) Side and (b) top views of SiH crystallized in a hexagonal structure with space group $P\bar{3}m1$ (No.164). (c) The bulk BZ and its corresponding surface BZ projected on the (100) surface.

where a_1 and a_2 are real parameters. Thus, the corresponding effective Hamiltonian retained to the leading order can be simplified to

$$H_{eff}(\mathbf{q}) = iaq_- \sigma_+ + H.c., \quad (6)$$

where a is a real parameter, and Eq. (6) indicates that the dispersion relation in the plane perpendicular to the NL is linear. According to the definition, the doubly degenerate nodal lines that are protected by C_{3v} are LNL.

For little group C_3 , the \mathcal{PT} symmetry satisfies the commutation relationship $[\mathcal{PT}, H]$. We assume that there is a set of basis $\{\psi, \mathcal{PT}\psi\}$ which are the eigenstates with common eigenvalue of Hamiltonian. Selecting a set of basis functions $\{-i(x + iy), i(x - iy)\}$ belong to two one-dimensional irreducible representations of C_3 , which meets $\psi_2 = \mathcal{PT}\psi_1(\{\psi_1, \psi_2\})$. So there is an essential degenerate NL. An arbitrary point on this path is invariant under the threefold rotation C_{3z} and \mathcal{PT} . The relevant representations are $\{\Gamma_2, \Gamma_3\}$, of which the basis are $\{-i(x + iy), i(x - iy)\}$. The matrix representations of the operators can be expressed in the above basis as

$$D(C_{3z}) = e^{2i\sigma_z\pi/3}, D(\mathcal{PT}) = \sigma_x \mathcal{K}, \quad (7)$$

where \mathcal{K} denotes the complex conjugation operator. The corresponding effective Hamiltonian reads

$$H_{eff}(\mathbf{q}) = \alpha q_- \sigma_+ + H.c., \quad (8)$$

where α is a complex parameter. As given in Eq.(8), the nodal lines protected by $C_3 + \mathcal{PT}$ are also LNL.

According to our model analysis, we find that SiH hosts the LNL phonons. As illustrated in Figs. 1(a) and 1(b), SiH crystallizes in a trigonal lattice with symmorphic space group $P\bar{3}m1$ (No. 164). The optimized lattice constants are $a = 3.861 \text{ \AA}$ and $c = 4.804 \text{ \AA}$. The hexagonal bulk BZ and its corresponding (100) surface BZ are shown in Fig. 1(c). There is a nodal line along the high symmetry line $K-H$ [see blue bold line in Fig. 1(c)].

As shown in Fig. 2(a), the phonon spectrum of SiH is plotted. It is noteworthy that we can find a doubly degenerate phonon band along the high symmetry line $K-H$ near 19 THz, which is contributed from the 8th and 9th phonon branches. These two crossing bands belong to states which have opposite eigenvalues $e^{2/3i\pi}$ of rotation symmetry operation C_{3z} , which protects the NL along $K-H$. Because the symmetries of the phonon momentum obey a C_{3v} point group along the $K-H$ direction, the doubly degenerate lines belong to a two-dimensional irreducible representation. The three-dimensional(3D) representation of two-dimensional phonon dispersion at any point on the nodal line is plotted in Fig. 2(b). There is a crossing of the two branches in the shape of a Dirac cone at the Q point in momentum space, which indicates that the dispersion relation is linear. These results from first-principles calculations agree well with our symmetry analysis. The band dispersion around a generic point also shows an obvious linear relationship in Fig. 2(c), indicating the existence of the LNL.

In Fig. 2(c), we plot the calculated phonon local density of states (LDOS) projected on the semi-infinite (100) surface of SiH. The topological drumhead surface states are clearly visible, which means that it is possible to observe surface states experimentally. As expected, the surface states begin at a crossing point on a high-symmetry line $\bar{\Gamma} - \bar{M}$ and terminate at a crossing point on another high symmetry line $\bar{A} - \bar{L}$. These results are consistent with our theoretical analysis and prove that the surface states come from the LNL phonons.

Quadratic nodal line

Our symmetry analysis shows that the QNL phonons are protected by eight different types of symmetries, including $C_2 + \mathcal{S}_4\mathcal{T}$, $C_{2v} + \mathcal{S}_4\mathcal{T}$, $C_3 + M_z\mathcal{T}$, $C_{3v} + M_z\mathcal{T}$, $C_4 + \mathcal{PT}$, C_{4v} , $C_6 + \mathcal{PT}$, and C_{6v} , respectively. Here, we take $C_{2v} + \mathcal{S}_4\mathcal{T}$ as an example, and more detailed results are provided in the supplementary materials (SM)[33].

Momentum with the C_{2v} symmetry on the line can be invariant under $\mathcal{S}_4\mathcal{T}$. So we can drive that $[\mathcal{S}_4\mathcal{T}, H]$. We

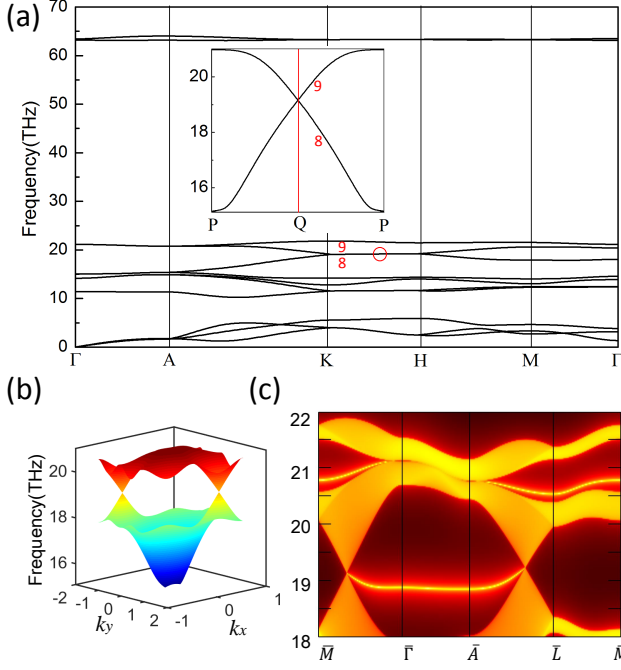


FIG. 2: (a) The phonon spectrum of SiH along the high-symmetry lines. P and Q are the midpoints of high symmetry lines Γ -A and K -H, respectively. (b) The 3D representation of the LNL phonons at any point on the nodal line. Here, we visualize them by selecting a node on the K -H at $k_z=0.2$. (c) LDOS projected on the semi-infinite (100) surface. Yellow areas denote the projections of bulk phonon branches, and yellow lines represent the nontrivial phonon surface states.

consider two states $\{\psi, \mathcal{S}_4\mathcal{T}\psi\}$, which are the eigenstates with the common eigenvalue of Hamiltonian. In addition, C_{2v} has two one-dimensional irreducible representations that are complex, and the relevant representations are $\{\Gamma_3, \Gamma_4\}$, of which the basis is $\{x, y\}$. Considering the operation $\mathcal{S}_4\mathcal{T}$, two one-dimensional irreducible representations are combined into a two-dimensional irreducible representation. So there is a doubly degenerate band. The little group contains two generators: the twofold rotation C_{2z} and the vertical mirror M_x . The matrix representations of the generators can be expressed on the above basis as

$$D(C_{2z}) = -\sigma_0, D(M_x) = \sigma_z. \quad (9)$$

Considering two operators C_{3z} and M_x which are acting on \mathbf{q} , the constraint Eq. (3) gives

$$\begin{aligned} f(q_+, q_-) &= f(-q_+, -q_-), \\ d(q_+, q_-) &= d(-q_+, -q_-), \\ f(q_+, q_-) &= f(-q_-, -q_+), \\ -d(q_+, q_-) &= d(-q_-, -q_+). \end{aligned} \quad (10)$$

Then we expand Eq. (10) and remain the lowest orders as

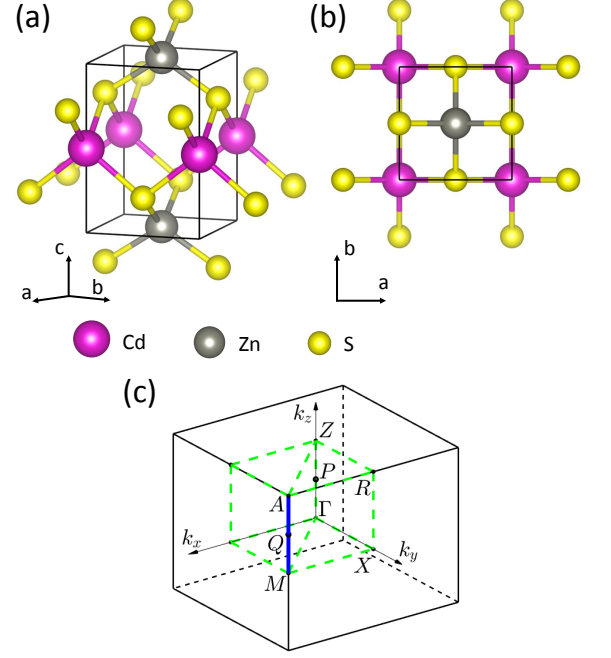


FIG. 3: Crystal structure and BZ. (a) Side and (b) top views of ZnCdS_2 with space group $P\bar{4}m2$ (No. 115). (c) The tetragonal bulk BZ.

$$\begin{aligned} f(\mathbf{q}) &= a_1(q_+^2 + q_-^2) + a_2q_+q_-, \\ d(\mathbf{q}) &= \alpha(q_+^2 - q_-^2). \end{aligned} \quad (11)$$

Thus, the corresponding effective Hamiltonian retained to the leading order can be simplified to

$$\begin{aligned} H_{eff}(\mathbf{q}) &= [a_1(q_+^2 + q_-^2) + a_2q_+q_-]\sigma_z \\ &+ \alpha(q_+^2 - q_-^2)\sigma_+ + H.c., \end{aligned} \quad (12)$$

which indicates that the dispersion relation in the plane perpendicular to the NL is quadratic. It is natural to conclude that the doubly degenerate phonon NLS protected by $C_{2v} + \mathcal{S}_4\mathcal{T}$ are QNL.

ZnCdS_2 is an ideal candidate to possess the QNL phonons. As illustrated in Figs. 3(a) and 3(b), ZnCdS_2 crystallizes in a tetragonal lattice with space group $P\bar{4}m2$ (No. 115). The optimized lattice constants are $a = 3.930$ Å and $c = 5.645$ Å. The tetragonal bulk BZ is shown in Fig. 3(c). We find that there is a NL along the high symmetry line M -A with $C_{2v} + \mathcal{S}_4\mathcal{T}$ symmetry.

As shown in Fig. 4(a), the phonon spectrum of ZnCdS_2 is plotted. It is noteworthy that we can find out a doubly degenerate phonon band along the high symmetry line M -A near 5 THz, which are contributed from the 5th and 6th phonon branches [highlighted in Fig. 4(b)]. Because the symmetries of the phonon momentum obey a C_{2v} point group along the M -A direction, the doubly degenerate line belongs to two one-dimension irreducible representations. These two crossing bands belong to states

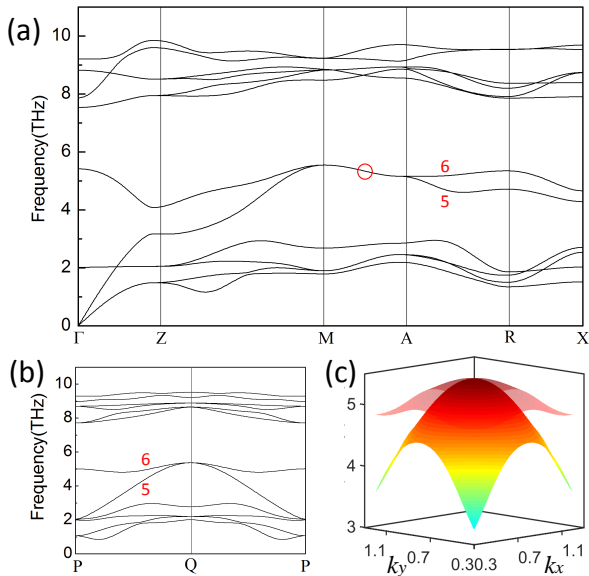


FIG. 4: (a) The phonon spectrum of ZnCdS₂ along the high-symmetry lines. (b) The band dispersion along the path P - Q - P (in direction perpendicular to the NL). P and Q are in the middle of Γ - Z and M - A , respectively. (c) The 3D view of the 5th and 6th bands restricted to the k_x - k_y plane at any point on the nodal line. Here, we visualize them by selecting a node on the M - A at $k_z=0.2$.

that have the opposite eigenvalues ± 1 of mirror reflection symmetry operation M_x , respectively, which protects the NL along the high symmetry line M - A . In Fig. 4(b), we can see an obvious quadratic dispersion relation around the Q point between the 5th and 6th branches. The 3D representation of two-dimensional phonon dispersion at any point on the nodal line is plotted in Fig. 4(c), and it also shows an obvious quadratic relation in the k_x - k_y plane. The evidence shows that the NL along M - A is indeed a QNL.

To further explore the topological properties of these NLs, the corresponding Berry phase distribution is considered. In general, the Berry phase of a closed path C in 3D BZ is defined as [34]

$$\gamma_C = \oint_C \mathbf{A}_n(\mathbf{q}) \cdot d\mathbf{q}, \quad (13)$$

where $\mathbf{A}_n(\mathbf{q}) = i\langle \psi_n(\mathbf{q}) | \nabla_{\mathbf{q}} | \psi_n(\mathbf{q}) \rangle$ is the Berry connection and $\psi_n(\mathbf{q})$ is the Bloch wave function of occupied bands. We select a closed circle centered at a generic point of the nodal line. Note that the circle lies on the plane perpendicular to the line and cannot cover another nodal line. Interestingly, we find that the Berry phase for the LNL phonons in SiH along the K - H is π , for QNL in ZnCdS₂ along M - A is 2π . More details are included in Table SI of the SM. The results show that the Berry phase are π for linear NLs, and 2π for QNLs.

CONCLUSIONS

In summary, using first-principles calculations and effective model analysis, we have systematically studied the symmetry-protected NL phonons in symmorphic space groups. All possible straight NL phonons have been uncovered, and our results show that the highest-order dispersion relation perpendicular to the NL is quadratic. Via symmetry analysis, we have found the existing NL phonons in symmorphic space groups according to the corresponding little groups. We thus offer a feasible way of finding topological NL materials.

This work is supported by the National Natural Science Foundation of China (NSFC, Grants No. 11974160), the Guangdong Natural Science Funds for Distinguished Young Scholars (No. 2017B030306008), the fund of the Guangdong Provincial Key Laboratory of Computational Science and Material Design (No.2019B030301001), and the Center for Computational Science and Engineering at Southern University of Science and Technology.

* Electronic address: xuh@sustech.edu.cn

- [1] M. Z. Hasan and C. L. Kane, Rev. Mod. Phys. **82**, 3045 (2010).
- [2] X. L. Qi and S. C. Zhang, Rev. Mod. Phys. **83**, 1057 (2011).
- [3] N. P. Armitage, E. J. Mele, and A. Vishwanath, Rev. Mod. Phys. **90**, 015001 (2018).
- [4] Z. Wang, Y. Sun, X. Q. Chen, C. Franchini, G. Xu, H. Weng, X. Dai, and Z. Fang, Phys. Rev. B **85**, 195320 (2012).
- [5] X. Wan, A. M. Turner, A. Vishwanath, and S. Y. Savrasov, Phys. Rev. B **83**, 205101 (2011).
- [6] H. Weng, C. Fang, Z. Fang, B. A. Bernevig, and X. Dai, Physical Review X **5**, 011029 (2015).
- [7] H. Wang, J. Ruan, and H. Zhang, Phys. Rev. B **99**, 075130 (2019).
- [8] Z.M. Yu, W. Wu, X. L. Sheng, Y. X. Zhao, and S. A. Yang, Phys. Rev. B **99**, 121106 (2019).
- [9] G. Bian, T.R. Chang, H. Zheng, S. Velury, S. Y. Xu, T. Neupert, C. K. Chiu, S. M. Huang, D. S. Sanchez, I. Belopolski, et al., Phys. Rev. B **93**, 121113 (2016).
- [10] C. Fang, Y. Chen, H. Y. Kee, and L. Fu, Phys. Rev. B **92**, 081201 (2015).
- [11] M. Hirayama, R. Okugawa, T. Miyake, and S. Murakami, Nature communications **8**, 1 (2017).
- [12] Z. Yan, R. Bi, H. Shen, L. Lu, S. C. Zhang, and Z. Wang, Physical Review B **96**, 041103 (2017).
- [13] Y. Huh, E. G. Moon, and Y. B. Kim, Phys. Rev. B **93**, 035138 (2016).
- [14] W. Deng, J. Lu, F. Li, X. Huang, M. Yan, J. Ma, and Z. Liu, Nature communications **10**, 1 (2019).
- [15] C. Zhong, Y. Chen, Y. Xie, S. A. Yang, M. L. Cohen, and S. B. Zhang, Nanoscale **8**, 7232 (2016).

- [16] W. Wu, Y. Liu, S. Li, C. Zhong, Z. M. Yu, X. L. Sheng, Y. X. Zhao, and S. A. Yang, *Phys. Rev. B* **97**, 115125 (2018).
- [17] Q. F. Liang, J. Zhou, R. Yu, Z. Wang, and H. Weng, *Phys. Rev. B* **93**, 085427 (2016).
- [18] S.B. Zhang and J. Zhou, *Phys. Rev. B* **101**, 085202 (2020).
- [19] P. Wang, L. Lu, and K. Bertoldi, *Phys. Rev. Lett.* **115**, 104302 (2015).
- [20] Q. Xie, J. Li, S. Ullah, R. Li, L. Wang, D. Li, Y. Li, S. Yunoki, and X. Q. Chen, *Phys. Rev. B* **99**, 174306 (2019).
- [21] Y. Liu, Y. Xu, S. C. Zhang, and W. Duan, *Phys. Rev. B* **96**, 064106 (2017).
- [22] Y. J. Jin, Z. J. Chen, B. W. Xia, Y. J. Zhao, R. Wang, and H. Xu, *Phys. Rev. B* **98**, 220103 (2018).
- [23] R. Süssstrunk and S. D. Huber, *Science* **349**, 47 (2015).
- [24] F. Liu, H. Y. Deng, and K. Wakabayashi, *Phys. Rev. B* **97**, 035442 (2018).
- [25] O. Stenull, C. L. Kane, and T. C. Lubensky, *Phys. Rev. Lett.* **117**, 068001 (2016).
- [26] Y. Liu, Y. Xu, and W. Duan, *National Science Review* **5**, 314 (2018).
- [27] R. Süssstrunk and S. D. Huber, *Science* **349**, 47 (2015).
- [28] S. H. Mousavi, A. B. Khanikaev, and Z. Wang, *Nature communications* **6**, 1 (2015).
- [29] C. He, X. Ni, H. Ge, X. C. Sun, Y. B. Chen, M. H. Lu, X. P. Liu, and Y. F. Chen, *Nature physics* **12**, 1124 (2016).
- [30] T. T. Zhang, H. Miao, Q. Wang, J. Q. Lin, Y. Cao, G. Fabbris, A. H. Said, X. Liu, H. C. Lei, Z. Fang, et al., *Phys. Rev. Lett.* **123**, 245302 (2019).
- [31] B. Peng, Y. Hu, S. Murakami, T. Zhang, and B. Monserrat, *Science advances* **6**, eabd1618 (2020).
- [32] J. Li, Q. Xie, J. Liu, R. Li, M. Liu, L. Wang, D. Li, Y. Li, and X. Q. Chen, *Phys. Rev. B* **101**, 024301 (2020).
- [33] See Supplemental Material for the computational method, the detailed symmetry and effective model analysis, the summary of space groups, which includes Refs. [35-44].
- [34] M. V. Berry, *Proceedings of the Royal Society of London. A. Mathematical and Physical Sciences* **392**, 45 (1984).
- [1] W. Kohn and L. J. Sham, *Physical review* **140**, A1133 (1965).
- [2] G. Kresse and J. Furthmüller, *Phys. Rev. B* **54**, 11169 (1996).
- [3] G. Kresse and J. Furthmüller, *Computational materials science* **6**, 15 (1996).
- [4] J. P. Perdew, K. Burke, and M. Ernzerhof, *Phys. Rev. Lett.* **77**, 3865 (1996).
- [5] J. P. Perdew, K. Burke, and M. Ernzerhof, *Phys. Rev. Lett.* **78**, 1396 (1997).
- [6] G. Kresse and D. Joubert, *Phys. Rev. B* **59**, 1758 (1999).
- [7] D. M. Ceperley and B. J. Alder, *Phys. Rev. Lett.* **45**, 566 (1980).
- [8] A. Togo and I. Tanaka, *Scripta Materialia* **108**, 1 (2015).
- [9] M. P. L. Sancho, J. M. L. Sancho, and J. Rubio, *Journal of Physics F: Metal Physics* **14**, 1205 (1984).
- [10] Q. Wu, S. Zhang, H. F. Song, M. Troyer, and A. A. Soluyanov, *Computer Physics Communications* **224**, 405 (2018).

Supplemental Material for “Straight nodal-line phonons in symmorphic space groups”

Calculation methods

All the calculations were based on the framework of density functional theory (DFT) [1] using the Vienna *ab-initio* Simulation Package (VASP) [2, 3]. The generalized gradient approximation (GGA) with the Perdew-Burke-Ernzerhof (PBE) formalism was employed for the exchange-correlation function [4, 5]. The projector augmented wave method was employed to treat core-valence interactions [6, 7]. For phonon spectra calculations, we used the PHONOPY code to construct the force constants matrices and generate the symmetry information [8]. The phonon surface states were calculated using the iterative Green function method [9] with the tight-binding model Hamiltonian carried out by the Wannier-Tools package [10].

Details of the $k \cdot p$ model

To understand the properties of the phonon NLs, we first show the nodal-line solution in terms of the two-band $k \cdot p$ effective Hamiltonian. Generally, the crossings of two phonon branches can be described by a 2×2 effective Hamiltonian, namely

$$H(\mathbf{q}) = d(\mathbf{q})\sigma_+ + d^*(\mathbf{q})\sigma_- + f(\mathbf{q})\sigma_z \quad (\text{S14})$$

where H is referenced to the frequency of an arbitrary point on the phonon NL, $d(\mathbf{q})$ represents a complex function, $f(\mathbf{q})$ represents a real function.

Linear nodal lines

Point group C_3 with \mathcal{PT}

Considering a double degenerate phonon band where the little group is C_3 . We know that point group C_3 has two one-dimensional irreducible representations which are complex conjugate to each other. Considering the symmetry of combined operator \mathcal{PT} , two one-dimensional irreducible representations can be combined into a two-dimensional irreducible representation. The basis functions are $\{-i(x + iy), i(x - iy)\}$ or $\{-(S_x + iS_y), (S_x - iS_y)\}$

To construct the $k \cdot p$ effective Hamiltonian around a generic point, we express the symmetry operators in the basis:

$$C_{3z} = \begin{pmatrix} e^{\frac{2i\pi}{3}} & 0 \\ 0 & e^{-\frac{2i\pi}{3}} \end{pmatrix}, C_{3z}^{-1} = \begin{pmatrix} e^{-\frac{2i\pi}{3}} & 0 \\ 0 & e^{\frac{2i\pi}{3}} \end{pmatrix}, \quad (\text{S15})$$

$$\mathcal{PT} = \begin{pmatrix} 0 & 1 \\ 1 & 0 \end{pmatrix} K, \mathcal{PT} = \begin{pmatrix} 0 & 1 \\ 1 & 0 \end{pmatrix} \mathcal{K},$$

where \mathcal{K} is the complex conjugation operator, and σ_i are the Pauli matrices with $i=0, x, y, z$. The Hamiltonian is required to be invariant under the symmetry transformations, namely,

$$D(R)H_{eff}(\mathbf{q})D^{-1}(R) = H_{eff}(R\mathbf{q}), \quad (\text{S16})$$

where R denotes the corresponding operator C_{3z} and \mathcal{PT} which are acting on \mathbf{q} . The constraint Eq. (S3) gives

$$\begin{aligned} f(q_+, q_-) &= f(e^{i2\pi/3}q_+, e^{-i2\pi/3}q_-), \\ e^{i4\pi/3}d(q_+, q_-) &= d(e^{i2\pi/3}q_+, e^{-i2\pi/3}q_-), \\ -f^*(q_+, q_-) &= f(q_+, q_-), \\ d(q_+, q_-) &= d(q_+, q_-). \end{aligned} \quad (\text{S17})$$

where $\sigma_{\pm} = (\sigma_x \pm i\sigma_y)/2$. Thus, the corresponding effective Hamiltonian retained to the lowest order of $f(\mathbf{q})$ and $d(\mathbf{q})$ can be simplified to

$$H_{eff} = a(q_+^3 - q_-^3)\sigma_z + \alpha q_- \sigma_+ + H.c., \quad (\text{S18})$$

where a is a real parameter and α is a complex parameter. Thus, we conclude that the doubly degenerate line at leading order is a linear NL.

Point group C_{3v}

Considering a double degenerate phonon band where the little group is C_{3v} . We know that point group C_{3v} have a two dimensional irreducible representation which corresponding to a double degenerate band. C_{3v} contains two generators: C_{3z}, M_x . The basis functions are $\{(S_x - iS_y), -(S_x + iS_y)\}$

To construct the $k \cdot p$ effective Hamiltonian around a generic point, we express the symmetry operators in the basis:

$$C_{3z} = \begin{pmatrix} e^{\frac{2i\pi}{3}} & 0 \\ 0 & e^{-\frac{2i\pi}{3}} \end{pmatrix}, C_{3z}^{-1} = \begin{pmatrix} e^{-\frac{2i\pi}{3}} & 0 \\ 0 & e^{\frac{2i\pi}{3}} \end{pmatrix}, \quad (\text{S19})$$

$$M_x = \begin{pmatrix} 0 & 1 \\ 1 & 0 \end{pmatrix}, M_x^{-1} = \begin{pmatrix} 0 & 1 \\ 1 & 0 \end{pmatrix},$$

The constraint Eq. (S3) gives

Point group C_2 with $S_4\mathcal{T}$

$$\begin{aligned}
f(q_+, q_-) &= f(e^{i2\pi/3}q_+, e^{-i2\pi/3}q_-), \\
e^{i4\pi/3}d(q_+, q_-) &= d(e^{i2\pi/3}q_+, e^{-i2\pi/3}q_-), \\
-f(q_+, q_-) &= f(-q_-, -q_+), \\
d^*(q_+, q_-) &= d(-q_-, -q_+).
\end{aligned} \tag{S20}$$

Thus, the corresponding effective Hamiltonian retained to the lowest order of $f(\mathbf{q})$ and $d(\mathbf{q})$ can be simplified to

$$H_{eff} = a_1(q_+^3 + q_-^3)\sigma_z + ia_2q_-\sigma_+ + H.c., \tag{S21}$$

where $a_{1,2}$ is a real parameter. Thus, we conclude that the doubly degenerate line at leading order is a linear NL.

Quadratic nodal lines

Point group C_{2v} with $S_4\mathcal{T}$

Considering a double degenerate phonon band where the little group is C_{2v} . We know that point group C_{2v} has two one-dimensional irreducible representations which are complex conjugate to each other. Considering the symmetry operator $S_4\mathcal{T}$, two one-dimensional irreducible representations can be combined into a two-dimensional irreducible representation. So there is a double degenerate band. C_{2v} contains two generators: C_{2z}, M_x . The basis functions are $\{x, y\}$.

To construct the $k \cdot p$ effective Hamiltonian around a generic point, we express the symmetry operators in the basis:

$$\begin{aligned}
C_{2z} &= \begin{pmatrix} -1 & 0 \\ 0 & -1 \end{pmatrix}, C_{2z}^{-1} = \begin{pmatrix} -1 & 0 \\ 0 & -1 \end{pmatrix}, \\
M_x &= \begin{pmatrix} 1 & 0 \\ 0 & -1 \end{pmatrix}, M_x^{-1} = \begin{pmatrix} 1 & 0 \\ 0 & -1 \end{pmatrix},
\end{aligned} \tag{S22}$$

The constraint Eq. (S3) gives

$$\begin{aligned}
f(q_+, q_-) &= f(-q_+, -q_-), \\
d(q_+, q_-) &= d(-q_+, -q_-), \\
f(q_+, q_-) &= f(-q_-, -q_+), \\
-d(q_+, q_-) &= d(-q_-, -q_+).
\end{aligned} \tag{S23}$$

Thus, the corresponding effective Hamiltonian retained to the lowest order of $f(\mathbf{q})$ and $d(\mathbf{q})$ can be simplified to

$$H_{eff}(\mathbf{q}) = [a_1(q_+^2 + q_-^2) + a_2q_+q_-]\sigma_z + \alpha(q_+^2 - q_-^2)\sigma_+ + H.c. \tag{S24}$$

where $a_{1,2}$ is a real parameter. Thus, we conclude that the doubly degenerate line at leading order is a QNL with an approximate chiral symmetry.

Considering a double degenerate phonon band where the little group is C_2 . Considering the time reversal symmetry, one-dimensional irreducible representations can be combined into a two-dimensional irreducible representation. So there is a double degenerate band. C_2 contains one generator: C_{2z} . The basis functions are $\{x, \mathcal{T}x\}$.

To construct the $k \cdot p$ effective Hamiltonian around a generic point, we express the symmetry operators in the basis:

$$C_{2z} = \begin{pmatrix} -1 & 0 \\ 0 & -1 \end{pmatrix}, C_{2z}^{-1} = \begin{pmatrix} -1 & 0 \\ 0 & -1 \end{pmatrix}, \tag{S25}$$

The constraint Eq. (S3) gives

$$\begin{aligned}
f(q_+, q_-) &= f(-q_+, -q_-), \\
d(q_+, q_-) &= d(-q_+, -q_-).
\end{aligned} \tag{S26}$$

Thus, the corresponding effective Hamiltonian retained to the lowest order of $f(\mathbf{q})$ and $d(\mathbf{q})$ can be simplified to

$$H_{eff}(\mathbf{q}) = (a_1q_+^2 + a_2q_-^2 + a_3q_+q_-)\sigma_z + (\alpha_1q_+^2 + \alpha_2q_-^2 + \alpha_3q_+q_-)\sigma_+ + H.c. \tag{S27}$$

where $a_{1,2,3}$ is a real parameter, $\alpha_{1,2,3}$ is a complex parameter. Thus, we conclude that the doubly degenerate line at leading order is a QNL with an approximate chiral symmetry.

Point group C_3 with $M_z\mathcal{T}$ symmetry

Consider a double degenerate phonon band where the little group is C_3 . We know that point group C_3 has two one-dimensional irreducible representations which are complex conjugate to each other. Considering the symmetry of combined operator $M_z\mathcal{T}$, two one-dimensional irreducible representations can be combined into a two-dimensional irreducible representation. So there is a double degenerate band. The basis functions are $\{-(S_x + iS_y), (S_x - iS_y)\}$

To construct the $k \cdot p$ effective Hamiltonian around a generic point, we express the two symmetry operators C_3 and $M_z\mathcal{T}$ in the basis:

$$\begin{aligned}
C_{3z} &= \begin{pmatrix} e^{\frac{2i\pi}{3}} & 0 \\ 0 & e^{-\frac{2i\pi}{3}} \end{pmatrix}, C_{3z}^{-1} = \begin{pmatrix} e^{-\frac{2i\pi}{3}} & 0 \\ 0 & e^{\frac{2i\pi}{3}} \end{pmatrix}, \\
M_z\mathcal{T} &= \sigma_x\mathcal{K} = \begin{pmatrix} 0 & 1 \\ 1 & 0 \end{pmatrix}\mathcal{K}, (M_z\mathcal{T})^{-1} = \sigma_x\mathcal{K} = \begin{pmatrix} 0 & 1 \\ 1 & 0 \end{pmatrix}\mathcal{K},
\end{aligned} \tag{S28}$$

The constraint Eq. (S3) gives

Point Group C_4 with \mathcal{PT} symmetry

$$\begin{aligned}
f(q_+, q_-) &= f(e^{i2\pi/3}q_+, e^{-i2\pi/3}q_-), \\
e^{i4\pi/3}d(q_+, q_-) &= d(e^{i2\pi/3}q_+, e^{-i2\pi/3}q_-), \\
-f^*(q_+, q_-) &= f(-q_+, -q_-), \\
d(q_+, q_-) &= d(-q_+, -q_-).
\end{aligned} \tag{S29}$$

Thus, the corresponding effective Hamiltonian retained to the lowest order of $f(\mathbf{q})$ and $d(\mathbf{q})$ can be simplified to

$$H_{eff}(\mathbf{q}) = a(q_+^3 + q_-^3)\sigma_z + \alpha q_+^2\sigma_+ + H.c.. \tag{S30}$$

Thus, we conclude that the doubly degenerate line at leading order is a QNL with an approximate chiral symmetry.

Point group C_{3v} with $M_z\mathcal{T}$ symmetry

Considering a double degenerate phonon band where the little group is C_{3v} . We know that point group C_{3v} has a two-dimensional irreducible representation which corresponds to a doubly degenerate band. C_{3v} contains two generators: C_{3z} , M_y . The basis functions are $\{(S_x - iS_y), -(S_x + iS_y)\}$

To construct the $k \cdot p$ effective Hamiltonian around a generic point, we express the three symmetry operators C_{3z} , M_y , and $M_z\mathcal{T}$ in the basis:

$$\begin{aligned}
C_{3z} &= \begin{pmatrix} e^{\frac{2i\pi}{3}} & 0 \\ 0 & e^{-\frac{2i\pi}{3}} \end{pmatrix}, C_{3z}^{-1} = \begin{pmatrix} e^{-\frac{2i\pi}{3}} & 0 \\ 0 & e^{\frac{2i\pi}{3}} \end{pmatrix}, \\
M_x &= \begin{pmatrix} 0 & 1 \\ 1 & 0 \end{pmatrix}, M_x^{-1} = \begin{pmatrix} 0 & 1 \\ 1 & 0 \end{pmatrix}, \\
M_z\mathcal{T} &= \sigma_x\mathcal{K} = \begin{pmatrix} 0 & 1 \\ 1 & 0 \end{pmatrix}\mathcal{K}, (M_z\mathcal{T})^{-1} = \sigma_x\mathcal{K} = \begin{pmatrix} 0 & 1 \\ 1 & 0 \end{pmatrix}\mathcal{K},
\end{aligned} \tag{S31}$$

The constraint Eq. (S3) gives

$$\begin{aligned}
f(q_+, q_-) &= f(e^{i2\pi/3}q_+, e^{-i2\pi/3}q_-), \\
e^{i4\pi/3}d(q_+, q_-) &= d(e^{i2\pi/3}q_+, e^{-i2\pi/3}q_-), \\
-f(q_+, q_-) &= f(-q_+, -q_+), \\
d^*(q_+, q_-) &= d(-q_+, -q_+) \\
-f^*(q_+, q_-) &= f(-q_+, -q_-), \\
d(q_+, q_-) &= d(-q_+, -q_-).
\end{aligned} \tag{S32}$$

Thus, the corresponding effective Hamiltonian retained to the lowest order of $f(\mathbf{q})$ and $d(\mathbf{q})$ can be simplified to

$$H_{eff}(\mathbf{q}) = a_1(q_+^3 + q_-^3)\sigma_z + a_2q_+^2\sigma_+ + H.c.. \tag{S33}$$

where $a_{1,2}$ is a real. Thus, we conclude that the doubly degenerate line at leading order is a QNL with an approximate chiral symmetry.

Considering a double degenerate phonon band where the little group is C_4 . We know that point group C_4 has two one-dimensional irreducible representations which are complex conjugate to each other. Considering the symmetry of combined operator \mathcal{PT} , two one-dimensional irreducible representations can be combined into a two-dimensional irreducible representation. So there is a double degenerate band. C_4 contains one generator: C_{4z} . The basis functions are $\{-i(x + iy), i(x - iy)\}$ or $\{-(S_x + iS_y), (S_x - iS_y)\}$

To construct the $k \cdot p$ effective Hamiltonian around a generic point, we express the symmetry operators C_{4z} , \mathcal{PT} in the basis:

$$\begin{aligned}
C_{4z} &= \begin{pmatrix} i & 0 \\ 0 & -i \end{pmatrix}, C_{4z}^{-1} = \begin{pmatrix} -i & 0 \\ 0 & i \end{pmatrix}, \\
\mathcal{PT} &= \begin{pmatrix} 0 & 1 \\ 1 & 0 \end{pmatrix}\mathcal{K}, (\mathcal{PT})^{-1} = \begin{pmatrix} 0 & 1 \\ 1 & 0 \end{pmatrix}\mathcal{K},
\end{aligned} \tag{S34}$$

The constraint Eq. (S3) gives

$$\begin{aligned}
f(q_+, q_-) &= f(iq_+, iq_-), \\
-d(q_+, q_-) &= d(iq_+, iq_-), \\
-f^*(q_+, q_-) &= f(q_+, q_-), \\
d(q_+, q_-) &= d(q_+, q_-).
\end{aligned} \tag{S35}$$

Thus, the corresponding effective Hamiltonian retained to the lowest order of $f(\mathbf{q})$ and $d(\mathbf{q})$ can be simplified to

$$H_{eff}(\mathbf{q}) = a(q_+^4 - q_-^4)\sigma_z + (\alpha_1q_+^2 + \alpha_2q_-^2)\sigma_+ + H.c.. \tag{S36}$$

where $\alpha_{1,2}$ is a complex. Thus, we conclude that the doubly degenerate line at leading order is a QNL with an approximate chiral symmetry.

Point Group C_{4v}

Considering a double degenerate phonon band where the little group is C_{4v} . We know that point group C_{4v} has a two-dimensional irreducible representation which corresponding to a double degenerate band. C_{4v} contains two generators: C_{4z} , M_x . The basis functions are $\{S_x, S_y\}$.

To construct the $k \cdot p$ effective Hamiltonian around a generic point, we express the symmetry operators in the basis:

$$\begin{aligned}
C_{4z} &= \begin{pmatrix} 0 & -1 \\ 1 & 0 \end{pmatrix}, C_{4z}^{-1} = \begin{pmatrix} 0 & 1 \\ -1 & 0 \end{pmatrix}, \\
M_x &= \begin{pmatrix} -1 & 0 \\ 0 & 1 \end{pmatrix}, M_x^{-1} = \begin{pmatrix} -1 & 0 \\ 0 & 1 \end{pmatrix},
\end{aligned} \tag{S37}$$

The constraint Eq. (S3) gives

$$\begin{aligned}
-f(q_+, q_-) &= f(iq_+, iq_-), \\
-d^*(q_+, q_-) &= d(iq_+, iq_-), \\
f(q_+, q_-) &= f(-q_-, -q_+), \\
-d(q_+, q_-) &= d(-q_-, -q_+).
\end{aligned} \tag{S38}$$

Thus, the corresponding effective Hamiltonian retained to the lowest order of $f(\mathbf{q})$ and $d(\mathbf{q})$ can be simplified to

$$H_{eff}(\mathbf{q}) = [a_1(q_+^2 + q_-^2) + a_2 q_+ q_-] \sigma_z + i a_3 (q_+^2 - q_-^2) \sigma_+ + H.c.. \tag{S39}$$

where $a_{1,2,3}$ is a real parameter. Thus, we conclude that the doubly degenerate line at leading order is a QNL with an approximate chiral symmetry.

Point Group C_6 with \mathcal{PT}

Considering a double degenerate phonon band where the little group is C_6 . We know that point group C_6 has two one-dimensional irreducible representations which are complex conjugate to each other. Considering the symmetry of combined operator \mathcal{PT} , two one-dimensional irreducible representations can be combined into a two-dimensional irreducible representation. So there is a double degenerate band. C_6 contains one generator: C_{6z} . The basis functions are $\{(x - iy)^2, (x + iy)^2\}$ or $\{-(S_x + iS_y), (S_x - iS_y)\}$

To construct the $k \cdot p$ effective Hamiltonian around a generic point, we express the two symmetry operators C_{6z} , \mathcal{PT} in the basis:

$$\begin{aligned}
C_{6z} &= \begin{pmatrix} e^{\frac{i\pi}{3}} & 0 \\ 0 & e^{-\frac{i\pi}{3}} \end{pmatrix}, C_{6z}^{-1} = \begin{pmatrix} e^{-\frac{i\pi}{3}} & 0 \\ 0 & e^{\frac{i\pi}{3}} \end{pmatrix}, \\
\mathcal{PT} = \sigma_x \mathcal{K} &= \begin{pmatrix} 0 & 1 \\ 1 & 0 \end{pmatrix} \mathcal{K}, (\mathcal{PT})^{-1} = \sigma_x \mathcal{K} = \begin{pmatrix} 0 & 1 \\ 1 & 0 \end{pmatrix} \mathcal{K},
\end{aligned} \tag{S40}$$

The constraint Eq. (S3) gives

$$\begin{aligned}
f(q_+, q_-) &= f(e^{i\pi/3} q_+, e^{-i\pi/3} q_-), \\
e^{i2\pi/3} d(q_+, q_-) &= d(e^{i\pi/3} q_+, e^{-i\pi/3} q_-), \\
-f^*(q_+, q_-) &= f(q_+, q_-), \\
d^*(q_+, q_-) &= d(q_+, q_-).
\end{aligned} \tag{S41}$$

Thus, the corresponding effective Hamiltonian retained to the lowest order of $f(\mathbf{q})$ and $d(\mathbf{q})$ can be simplified to

$$H_{eff}(\mathbf{q}) = a(q_+^6 - q_-^6) \sigma_z + \alpha q_+^2 \sigma_+ + H.c.. \tag{S42}$$

Thus, we conclude that the doubly degenerate line at leading order is a QNL with an approximate chiral symmetry.

Point group C_{6v}

Considering a double degenerate phonon band where the little group is C_{6v} . We know that point group C_{6v} has a two-dimensional irreducible representation which corresponding a double degenerate band. C_{6v} contains two generators: C_{6z}, M_x . And the basis functions are $\{(S_x - iS_y), -(S_x + iS_y)\}$

To construct the $k \cdot p$ effective Hamiltonian around a generic point, we express the symmetry operators in the basis:

$$\begin{aligned}
C_{6z} &= \begin{pmatrix} e^{\frac{i\pi}{3}} & 0 \\ 0 & e^{-\frac{i\pi}{3}} \end{pmatrix}, C_{6z}^{-1} = \begin{pmatrix} e^{-\frac{i\pi}{3}} & 0 \\ 0 & e^{\frac{i\pi}{3}} \end{pmatrix}, \\
M_x &= \begin{pmatrix} 0 & 1 \\ 1 & 0 \end{pmatrix}, M_x^{-1} = \begin{pmatrix} 0 & 1 \\ 1 & 0 \end{pmatrix},
\end{aligned} \tag{S43}$$

The constraint Eq. (S3) gives

$$\begin{aligned}
f(q_+, q_-) &= f(e^{i\pi/3} q_+, e^{-i\pi/3} q_-), \\
e^{i2\pi/3} d(q_+, q_-) &= d(e^{i\pi/3} q_+, e^{-i\pi/3} q_-), \\
-f(q_+, q_-) &= f(-q_-, -q_+), \\
d^*(q_+, q_-) &= d(-q_-, -q_+).
\end{aligned} \tag{S44}$$

Thus, the corresponding effective Hamiltonian retained to the lowest order of $f(\mathbf{q})$ and $d(\mathbf{q})$ can be simplified to

$$H_{eff}(\mathbf{q}) = a_1(q_+^6 - q_-^6) \sigma_z + a_2 q_+^2 \sigma_+ + H.c.. \tag{S45}$$

where $a_{1,2}$ is a real parameter. Thus, we conclude that the doubly degenerate line at leading order is a QNL with an approximate chiral symmetry.

* Electronic address: xuh@sustech.edu.cn

- [1] W. Kohn and L. J. Sham, Physical review **140**, A1133 (1965).
- [2] G. Kresse and J. Furthmüller, Phys. Rev. B **54**, 11169 (1996).
- [3] G. Kresse and J. Furthmüller, Computational materials science **6**, 15 (1996).

- [4] J. P. Perdew, K. Burke, and M. Ernzerhof, Phys. Rev. Lett. **77**, 3865 (1996).
- [5] J. P. Perdew, K. Burke, and M. Ernzerhof, Phys. Rev. Lett. **78**, 1396 (1997).
- [6] G. Kresse and D. Joubert, Phys. Rev. B **59**, 1758 (1999).
- [7] D. M. Ceperley and B. J. Alder, Phys. Rev. Lett. **45**, 566 (1980).
- [8] A. Togo and I. Tanaka, Scripta Materialia **108**, 1 (2015).
- [9] M. P. L. Sancho, J. M. L. Sancho, and J. Rubio, Journal of Physics F: Metal Physics **14**, 1205 (1984).
- [10] Q. Wu, S. Zhang, H.-F. Song, M. Troyer, and A. A. Soluyanov, Computer Physics Communications **224**, 405 (2018).

Nodal lines Table

Table S2: List of all possible NLs stabilized by point group symmetry. Location represents a high symmetry line with double degenerate nodal lines, and little group represents the corresponding wave vector group.

space group	location	little group	basis function	berry phase	generator
147	(0,0,w)	C_3	$\{-i(x+iy), i(x-iy)\}$	π	C_{3z}, \mathcal{PT}
147	(1/3,1/3,w)	C_3	$\{-i(x+iy), i(x-iy)\}$	π	C_{3z}, \mathcal{PT}
148	(w,w,w)	C_3	$\{-i(x+iy), i(x-iy)\}$	π	C_{3z}, \mathcal{PT}
156	(0,0,w)	C_{3v}	$\{(S_x - iS_y), -(S_x + iS_y)\}$	π	C_{3z}, M_x
157	(0,0,w)	C_{3v}	$\{(S_x - iS_y), -(S_x + iS_y)\}$	π	C_{3z}, M_x
157	(1/3,1/3,w)	C_{3v}	$\{(S_x - iS_y), -(S_x + iS_y)\}$	π	C_{3z}, M_x
157	(-1/3,-1/3,w)	C_{3v}	$\{(S_x - iS_y), -(S_x + iS_y)\}$	$-\pi$	C_{3z}, M_x
160	(w,w,w)	C_{3v}	$\{(S_x - iS_y), -(S_x + iS_y)\}$	π	C_{3z}, M_x
162	(0,0,w)	C_{3v}	$\{(S_x - iS_y), -(S_x + iS_y)\}$	π	$C_{3z}, M_x, \mathcal{PT}$
162	(1/3,1/3,w)	C_{3v}	$\{(S_x - iS_y), -(S_x + iS_y)\}$	π	$C_{3z}, M_x, \mathcal{PT}$
164	(0,0,w)	C_{3v}	$\{(S_x - iS_y), -(S_x + iS_y)\}$	π	$C_{3z}, M_x, \mathcal{PT}$
164	(1/3,1/3,w)	C_3	$\{-i(x+iy), i(x-iy)\}$	π	C_{3z}, \mathcal{PT}
166	(0,0,w)	C_{3v}	$\{(S_x - iS_y), -(S_x + iS_y)\}$	π	$C_{3z}, M_x, \mathcal{PT}$
175	(1/3,1/3,w)	C_3	$\{-i(x+iy), i(x-iy)\}$	π	C_{3z}, \mathcal{PT}
183	(1/3,1/3,w)	C_{3v}	$\{(S_x - iS_y), -(S_x + iS_y)\}$	π	C_{3z}, M_x
189	(1/3,1/3,w)	C_{3v}	$\{(S_x - iS_y), -(S_x + iS_y)\}$	π	C_{3z}, M_x
189	(-1/3,-1/3,w)	C_{3v}	$\{(S_x - iS_y), -(S_x + iS_y)\}$	$-\pi$	C_{3z}, M_x
191	(1/3,1/3,w)	C_{3v}	$\{(S_x - iS_y), -(S_x + iS_y)\}$	π	$C_{3z}, M_x, \mathcal{PT}$
200	(w,w,w)	C_3	$\{-i(x+iy), i(x-iy)\}$	π	C_{3z}, \mathcal{PT}
202	(w,w,w)	C_3	$\{-i(x+iy), i(x-iy)\}$	π	C_{3z}, \mathcal{PT}
204	(w,w,w)	C_3	$\{-i(x+iy), i(x-iy)\}$	π	C_{3z}, \mathcal{PT}
215	(w,w,w)	C_{3v}	$\{(S_x - iS_y), -(S_x + iS_y)\}$	π	C_{3z}, M_x
216	(w,w,w)	C_{3v}	$\{(S_x - iS_y), -(S_x + iS_y)\}$	π	C_{3z}, M_x
217	(w,w,w)	C_{3v}	$\{(S_x - iS_y), -(S_x + iS_y)\}$	π	C_{3z}, M_x
221	(w,w,w)	C_{3v}	$\{(S_x - iS_y), -(S_x + iS_y)\}$	π	$C_{3z}, M_x, \mathcal{PT}$
225	(w,w,w)	C_{3v}	$\{(S_x - iS_y), -(S_x + iS_y)\}$	π	$C_{3z}, M_x, \mathcal{PT}$
229	(w,w,w)	C_{3v}	$\{(S_x - iS_y), -(S_x + iS_y)\}$	π	$C_{3z}, M_x, \mathcal{PT}$
81	(0,0,w)	C_2	$\{x, \mathcal{T}x\}$	2π	$C_2, \mathcal{S}_4\mathcal{T}$
83	(0,0,w)	C_4	$\{-i(x+iy), i(x-iy)\}$	2π	C_{4z}, \mathcal{PT}
83	(1/2,1/2,w)	C_4	$\{-i(x+iy), i(x-iy)\}$	2π	C_{4z}, \mathcal{PT}
87	(w,w,-w)	C_4	$\{-i(x+iy), i(x-iy)\}$	2π	C_{4z}, \mathcal{PT}
99	(0,0,w)	C_{4v}	$\{S_x, S_y\}$	2π	C_{4z}, M_x
99	(1/2,1/2,w)	C_{4v}	$\{S_x, S_y\}$	2π	C_{4z}, M_x
107	(w,w,-w)	C_{4v}	$\{S_x, S_y\}$	2π	C_{4z}, M_x
111	(0,0,w)	C_{2v}	$\{x, y\}$	2π	$C_{2z}, M_x, \mathcal{S}_4\mathcal{T}$
111	(1/2,1/2,w)	C_{2v}	$\{x, y\}$	2π	$C_{2z}, M_x, \mathcal{S}_4\mathcal{T}$
115	(0,0,w)	C_{2v}	$\{x, y\}$	2π	$C_{2z}, M_x, \mathcal{S}_4\mathcal{T}$
115	(1/2,1/2,w)	C_{2v}	$\{x, y\}$	2π	$C_{2z}, M_x, \mathcal{S}_4\mathcal{T}$
119	(w,w,-w)	C_{2v}	$\{x, y\}$	2π	$C_{2z}, M_x, \mathcal{S}_4\mathcal{T}$
121	(w,w,-w)	C_{2v}	$\{x, y\}$	2π	$C_{2z}, M_x, \mathcal{S}_4\mathcal{T}$
123	(0,0,w)	C_{4v}	$\{S_x, S_y\}$	2π	$C_{4z}, M_x, \mathcal{PT}$
123	(1/2,1/2,w)	C_{4v}	$\{S_x, S_y\}$	2π	$C_{4z}, M_x, \mathcal{PT}$
139	(w,w,-w)	C_{4v}	$\{S_x, S_y\}$	2π	$C_{4z}, M_x, \mathcal{PT}$
174	(0,0,w)	C_3	$\{-i(x+iy), i(x-iy)\}$	2π	$C_3, M_z\mathcal{T}$
175	(0,0,w)	C_6	$\{(x-iy)^2, (x+iy)^2\}$	2π	$C_6, M_z\mathcal{T}, \mathcal{PT}$
183	(0,0,w)	C_{6v}	$\{(S_x - iS_y), -(S_x + iS_y)\}$	2π	C_{6z}, M_x
187	(0,0,w)	C_{3v}	$\{(S_x - iS_y), -(S_x + iS_y)\}$	2π	$C_{3z}, M_x, M_z\mathcal{T}$
189	(0,0,w)	C_{3v}	$\{(S_x - iS_y), -(S_x + iS_y)\}$	2π	$C_{3z}, M_x, M_z\mathcal{T}$
191	(0,0,w)	C_{6v}	$\{(S_x - iS_y), -(S_x + iS_y)\}$	2π	$C_{6z}, M_x, \mathcal{PT}$
215	(1/2,1/2,w)	C_{2v}	$\{x, y\}$	2π	$C_{2z}, M_x, \mathcal{S}_4\mathcal{T}$
215	(0,w,0)	C_{2v}	$\{x, y\}$	2π	$C_{2z}, M_x, \mathcal{S}_4\mathcal{T}$
216	(w,w,0)	C_{2v}	$\{x, y\}$	2π	$C_{2z}, M_x, \mathcal{S}_4\mathcal{T}$
217	(w,-w,w)	C_{2v}	$\{x, y\}$	2π	$C_{2z}, M_x, \mathcal{S}_4\mathcal{T}$
221	(1/2,1/2,w)	C_{4v}	$\{S_x, S_y\}$	2π	$C_{4z}, M_x, \mathcal{PT}$
221	(0,w,0)	C_{4v}	$\{S_x, S_y\}$	2π	$C_{4z}, M_x, \mathcal{PT}$
225	(w,w,0)	C_{4v}	$\{S_x, S_y\}$	2π	$C_{4z}, M_x, \mathcal{PT}$
229	(w,-w,w)	C_{4v}	$\{S_x, S_y\}$	2π	$C_{4z}, M_x, \mathcal{PT}$